Catalytic Wet Oxidating Fulvic Acid By Zero-Valent Copper Chitosan Activated Carbon Ball: Plackett-Buiman Design and Response Surface Modeling Optimization

Chaofei Song
Beijing University of Technology
Yue Lv
Beijing University of Technology
Xia Qin (qinxia@bjut.edu.cn)
Beijing University of Technology
Jiaxin Cui
Beijing University of Technology
Chengrui Guo
Beijing University of Technology
Kaghembega Steve-Harold
Beijing University of Technology

Research Article

Keywords: Zero-valent copper, Fulvic acid, catalytic wet oxidation, Plackett-Buiman, Response surface methodology model

Posted Date: January 7th, 2021

DOI: https://doi.org/10.21203/rs.3.rs-132991/v1

Version of Record: A version of this preprint was published at Scientific Reports on July 7th, 2021. See the published version at https://doi.org/10.1038/s41598-021-92789-6.

Catalytic wet oxidating fulvic acid by zero-valent copper chitosan activated carbon ball: Plackett-Buiman design and response surface modeling optimization

Chaofei Song[1], Xia Qin[1,*], Yue Lv[1], Chengrui Guo[1],Jiaxin Cui[1], Kaghembega Wendkuuni Steve-Harold[1]

1 Faculty of environment and life, Beijing University Of Technology, Beijing, 100124,China.
*Corresponding author:Tel.: +86 15011283641; E-mail address:qinxia@bjut.edu.cn.

Abstract

In this paper, the active component zero-valent copper (ZVC) supported by chitosan activated carbon ball (CTS-ACB) (i.e. ZVC/CTS-ACS catalyst) was successfully prepared. The characterization results showed obvious characteristics of activated carbon and zero-valent copper. The catalyst was used to degrade fulvic acid (FA) in catalytic wet oxidation(CWO) system. The two significant factors acidity and temperature were found with the statistical tool Plackett-Buimanhe(PB) in CWO for FA removal. Then the response surface methodology(RSM) model was used to optimize the experimental conditions in order to obtain the optimal FA removal rate. With the optimal experimental parameters, that is, a temperature of 94°C and an acidity of 3.8, the average maximum removal rate of FA was 93.02%, which was in agreement with the expected result of the model 93.86%, indicating that the model is well established. The comparison of catalytic performance showed that the addition of catalyst ZVC / CTS-ACS could increase the removal rate of FA, colour number(CN) and TOC by 93.6%, 83.5% and 81.9% respectively. The utilization of ZVC can greatly increase the mineralization rate of FA , which indicates the high catalytic activity and minerazation of the catalyst.

Keywords:Zero-valent copper · Fulvic acid · catalytic wet oxidation · Plackett-Buiman · Response surface methodology model

Introduction

Fulvic acid (FA), which is generally resistant to microbial degradation, is found in both natural waters and wastewater(14,18). According to Wang, Zhao and Wong (21, 22,26), in the chlorination stage of the water treatment FA and chlorine may produce a by-product trihalomethane whose strong carcinogenic and strong mutagenic properties seriously endanger human health. Moreover, FA contains a large number of oxygen-containing functional groups (phenolic hydroxyl groups, carboxyl groups, carbonyl groups, etc.) and has strong complexation with heavy metal ions, which increases the toxicity and handling difficulty of wastewater(3). The traditional microbial method has obvious effect on the removal of biodegradable organic matter in wastewater, but has a poor effect on the treatment of refractory organic pllutants including FA(10).

In in the past ten years, the Catalytic Wet Hydrogen Peroxide Oxidation (CWPO) process, especially

the process of using either carbon materials or zero-valent metals as catalysts, has attracted considerable attention(27,13,8,23). CWPO is effective in removing organic compounds, by which organic matter is converted into biodegradable products, even directly mineralized into CO_2 and H_2O(2,5). The advantages of high efficiency and low secondary pollution make CWPO process more attractive for the treatment of complex organic wastewater(16,17). However, research on combining carbon materials and zero-valent metals into one catalyst is rare.

Traditionally, the CWPO experimental conditions have been optimized by several single factor or orthogonal experiments, which require a large amount of work and the optimal conditions can be found only inside the chosen experiment points. In addition, the traditional methods also ignore the interaction among some parameters[6]. Plackett-Burman (PB)(15,24) design is a statistical method for screening multi-factors, through data analysis to find the key factors that have the greatest impact on the target value. The statistical experiment design of the response surface method (RSM) can optimize all the influence parameters, thus eliminating the limitations of single factor optimization, and finding the optimal target response point outside the set condition interval(4).

The purpose of this study was to evaluate the efficiency of removing FA from aqueous solution in the CWPO process with zero-valent copper chitosan activated carbon ball (ZVC/CTS-ACB) as catalyst . The RSM coupled with PB was used to optimize the parameters of CWPO experiment. The catalyst was prepared and the catalytic performance in CWPO was investigated in comparison with the other degradation processes in removal of FA.

Materials and methods

Materials

FA was purchased from Cool Chemical Technology Corporation (Beijing). The appearance color of the FA solution is from dark yellow to light yellow depending on the concentration. Chitosan was supplied by Jinan Haidebei Marine Bioengineering, whose Deacetylation Degree≥85%, Particle≥40 Mesh and viscosity=200mpas. All other agents were of analytical grade and purchased from Beijing Chemical Plant. The pH of the FA solution was adjusted byadding H_2SO_4 or NaOH. All the water used in the experiment was deionized water, from a Millipore-Q system with a resistance of 18.2 MΩ.

Preparation and characteristics of ZVC/CTS-ACB

The preparation of ZVC/CTS-ACB was carried out according to the following steps: (1) Preparation of chitosan gel: 7.25 g of $CuNO_4 \cdot 3H_2O$ was weighed and dissolved in 960 ml of deionized water, at the same time 0.1g of citric acid was added, and then 30 g of chitosan was weighed and dispersed in a copper nitrate solution to form a suspension. 40 ml of acetic acid was added while stirring quickly and uniformly until forming a gel, which allowed to stand overnight to discharge air bubbles. (2) The gel was added dropwise to a 3.75 to 5 wt% sodium hydroxide solution using a syringe, then was allowed to stand for 4-6 hours. (3) After washing to neutral and drying at 60~100°C for one night, the precursor was kept at 800~850°C for 2h~5h in an inert gas tube furnace to complete its carbonization and become activated carbon ball. (4)The activated carbon ball was rinsed several

times in ethanol and deionized water, and then dried at 80°C to remove moisture. X-ray diffraction (XRD) and scanning electron microscopy (SEM) analysis were performed on the ZVC/CTS-ACB catalyst, as shown in Fig 1 and Fig 2.

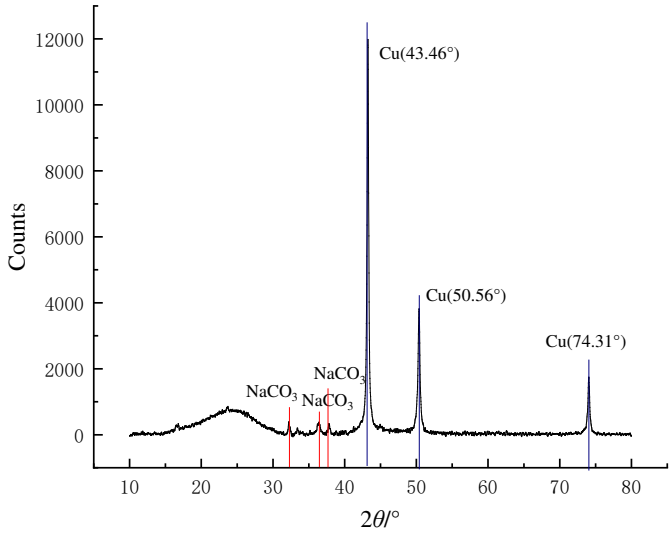

Fig. 1 XRD pattern of ZVC/CTS-ACB

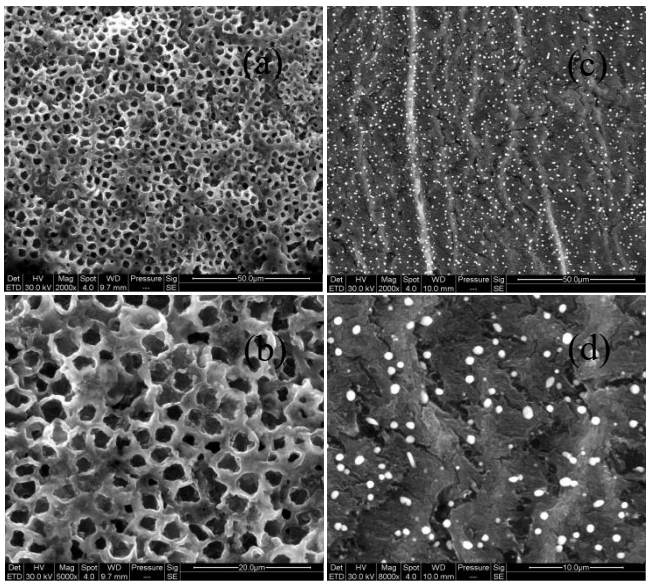

Fig. 2 SEM micrograph of external and internal cross-section of ZVC/CTS-ACB

(a.outer surface is magnified 2,000 times, b.outer surface is magnified 5,000 times, c.inner cut surface is magnified 2,000 times, d inner cut surface is magnified 8,000 times)

The result of X-ray diffraction analysis in Fig. 1 showed a large abundance of amorphous state at 20~30°, which is in line with the characteristics of activated carbon(7). There are some low continuous small peaks between 30-40° which are characteristic peaks of Na_2CO_3 produced by the NaOH in curing stage in the catalyst preparation. The other three distinct peaks tend to point to

metallic copper with a cubic structure (JCPDS 85-1326). The diffraction peaks at 43.46°, 50.56°, and 74. 31°are attributed to the reflection of the (111), (200) and (220) faces of the zero-valent copper(25), respectively. The result of Scanning electron microscopy analysis in Fig.2 showed a porous network structure on the surface of the catalyst, and the cross-sectional view showed uniform distribution of copper microcrystalline particles in the interior. Therefore, it can be concluded from these analytical characterizations that a large amount and uniform of zero-valent copper active component was successfully loaded on the activated carbon ball.

Experimental studies

The CWPO reaction was carried out in a reactor that can control the temperature. The pH of water sample was adjusted by H_2SO_4 and NaOH, and an appropriate amount of ZVC/CTS-ACB was added to the water sample. When the reaction temperature reached the set temperature, 30% of H_2O_2 was dropped into the reactor through the transfer pipe to make hydrogen oxide fully contact the catalyst to produce strong oxidizing free radicals(12), such as $\cdot OH$, $\cdot O_2$, etc. These free radicals can oxidize organics into small molecular organics and even to H_2O and CO_2. Samples were taken from the reaction effluent under different conditions. MnO_2 was added to the sample to prevent the influence of excess H_2O_2 on the detection results, and then the sample was filtered through a 0.45 um membrane for subsequent test results.

Analytical methods

The surface and profile morphology of the catalyst and the distribution of the supported metal crystals were observed using SEM (FEI Quanta 200). The active crystal phase composition of the catalyst was identified by XRD (D8 Advance type). The pH was measured by using a pH meter (pHs-3C type). The total organic carbon (TOC) of the influent and effluent was analyzed using a total organic carbon analyzer (TOC-5000A, Shimadzu, Japan), and the mineralization rate (α, %) was calculated by Eq 1.

$$(\alpha = \frac{TOC_0 - TOC}{TOC_0} \times 100\% \quad 1)$$

Where TOC_0 is the initial concentration and TOC is the effluent concentration.

The absorbance of FA was measured at a wavelength of 254 nm using an ultraviolet-visible spectrophotometer (Hitachi U-3900). The removal rate (β, %) of the FA(9) is calculated by Eq 2.

$$(\beta = \frac{UV_{254(0)} - UV_{254}}{UV_{254(0)}} \times 100\% \quad 2)$$

The color number of FA can be calculated and analyzed by UV-vis[19]. Since the visible region of the leachate spectrum showed no limited absorption maxima, the colour number (CN) as defined by Eq. (3) was used to characterise colour. CN relies on the measurement of the spectral absorption coefficient (SAC) in the visible range at wavelengths of 436, 525 and 620 nm. SAC is determined

by the absorption value (Abs) divided by a cell of thickness x shown in Eq 4.

$$(CN = \frac{SAC_{436}^2 + SAC_{525}^2 + SAC_{620}^2}{SAC_{436} + SAC_{525} + SAC_{620}} \quad 3)$$

$$SAC_i = \frac{Abs_i}{x} \quad 4)$$

The CN removal rate (γ, %) of FA is calculated by Eq 5.

$$(\gamma = \frac{CN_i - CN_0}{CN_i} \times 100\% \quad 5)$$

Plackett-Burman and response surface methodology

The Design Expert Software (version 8.0) was used for the experiment design and data analysis. Plackett-Burman(PB) coupled with central composite design response surface methodology(CCD-RSM) were used to evaluate and optimize the impact factors. Taking the removal rate of FA as the response target, two steps were used to optimize the experimental factors: Firstly, the PB experimental design was used to select the factors that greatly influenced the response, then the central composite design (CCD) of RSM is used to find the optimum experimental conditions. During the experiment period, the CWPO was performed to degrade FA according to the designed conditions, the absorbance values of the FA samples before and after the reaction were measured at a wavelength of 254 nm, and the removal rate of the target fulvic acid was calculated by the formula (2). After the experiment, the second-order response surface model equation was obtained and the optimal experimental conditions were determined by PB and CCD-RSM, and finally the optimal conditons were verified by conducting three repetitive tests.

Plackett-Burman experiment

The Plackett-Burman experimental design was proposed by Plackett and Burman in 1946. It was based on the principle of incompletely balanced plates. At most (N - 1) variables (N was generally a multiple of 4) could be studied by N experiments(15). During the experiment, dummy variables are usually reserved as error analysis. Each variable has two levels, high and low, marked as (+) and (-) respectively.

The Plackett-Burman design of the CWPO experiment was shown in Table 1. The seven main factors of the FA degradation experiment were screened, plus four dummy variables. Each variable was determined at two levels (+) and (-), and a total of 12 experiments were conducted to determine the impact factos.

Table 1 Factors of PB design experment

Variable	X1:A	X2:B	X3:C	X4:D	X5:E	X6:F	X7:G	X8, X9, X10, X11(H, I, J, K)
Factors	Temperature/℃	Initial volume/ml	Initial FA concentration/mg·L^{-1}	Time/min	H_2O_2/mmol	(ZVC/CTS-ACB)/g·L^{-1}	acidity	—
High level (+)	90	250	100	45	10	3	4	—
Low level (-)	60	500	200	90	20	5	7	—

Response surface methodology

The Central Composite Design (CCD) developed by Box and Wilson is a commonly used response surface design method , with which a optimal fitted model can be obtained with a minimum of experiments. The second-order empirical model is generally used to characterize the response behavior of variables. $Y = \beta_0 + \sum_{i=1}^{k} \beta_i X_i + \sum_{i=1}^{j-1} \sum_{j=1}^{k} \beta_{ij} X_i X_j + \sum_{i=1}^{k} \beta_{ii} X_i^2$

Where: Y represents the system response; β_0, βi, βii are the offset term, linear offset and second-order offset coefficient respectively; βij is the interaction coefficient; Xi is the horizontal value of each factor.

Comparative Experiment of Catalytic Performance

In order to better understand the role of the catalyst(ZVC/CTS-ACB) in CWPO process, the UV_{254}, TOC and CN removal efficiency of FA was investigated in various CWPO systems.

Results and discussion

Plackett-Burman experimental design results and analysis

The results of 12 runs of the FA removal experiments were shown in Table 2. The analysis of variance (ANOVA) results were showed in Table 3 with a list of significant differences of each factor impact.

Table 2 Plackett-Burman experiment design and response values

Run	Factor: A	Factor: B	Factor: C	Factor: D	Factor: E	Factor: F	Factor: G	Response(%)
1	-	+	-	-	+	-	+	37.77
2	+	+	-	+	+	+	-	84.59
3	+	-	+	+	-	-	+	51.13
4	+	+	-	-	+	-	+	48.41
5	+	-	-	-	-	+	+	45.59
6	-	+	+	+	-	+	+	34.38
7	-	-	+	-	+	+	-	74.54
8	+	-	+	+	+	-	-	83.11
9	-	-	-	+	+	+	+	41.07
10	-	-	-	-	-	-	-	73.32
11	-	+	-	+	-	-	-	78.29
12	+	+	+	-	-	+	-	81.26

Table 3 ANOVA results

Source	Mean Square	F Value	Value	Remarks
Model	525.97	51.46	0.0040	significant
A	197.94	19.37	0.0218	significant
B	1.66	0.16	0.7141	Not significant
C	6.21	0.61	0.4926	Not significant
D	8.32	0.81	0.4357	Not significant
E	2.18	0.21	0.6753	Not significant
F	8.32	0.81	0.4335	Not

				significant
G	338.98	37.13	0.0041	significant

As shown in Table 3, the Model F-value of 51.46 proves the model is significant. There is only a <0. 004 chance that the F-value of the model is the result of noise. In this case, A, G are significant model terms. Values greater than 0. 1000 indicate the model terms are not significant. It could be concluded that the only temperature and acidity factors have significant effects on the target values among the seven factors considered. Therefore, two significant factors, temperature and acidity, were selected for the following central combination design.

CCD optimization design results and response surface analysis

The CCD was conducted for the two important factors (Temperature and acidity) selected by Plackett-Buiman with other non-critical factors fixed: Initial volume=250ml, Initial concentration=100mg·L-1, Time = 60 min, H_2O_2 = 20 mmol, (ZVC/CTS-ACB) = 3 $g \cdot L^{-1}$. The CWPO degradation FA experiment was performed according to the designed conditions, and the target response value was calculated.

Model fitting and analysis of variance

Table 4 shows the conditons of 13 runs and the value of FA removal rates. Evaluation of data in this table provided a second-order polynominal [equation 3 below] to express the relationship between FA removal efficiency and the experimental parameters.

$$Y = 80.25 + 15.98A + 20.28B - 6.64A^2 - 25.70B^2 \quad (3)$$

Where: Y is the target response value, ie the removal of the FA. A and B represent temperature and acidity, respectively.

Table 4 CCD experimental design table

Run	1	2	3	4	5	6	7	8	9	10	11	12	13
Factor A:Temperature(°C)	90	90	70	50	70	70	98	42	70	70	70	70	50
Factor B:acidity	5.0	1.0	3.0	1.4	1.2	5.8	1.2	5.8	3.0	3.0	3.0	3.0	5.0
Response: removal rate of FA (%)	80.78	44.03	84.78	34.89	30.44	62.99	91.80	41.45	80.56	74.94	84.78	80.80	46.60

Table 5 shows the results of the RSM model fitting in the form of an analysis of variance (ANOVA). According to the table, the high F-value (F value = 29.21) and the very low probability values (P value < 0.0001) indicate the model obtained is highly significant. At the same time, the F value of the missing term is 4.66, indicating that the missing term has no significant effect, so the established model can be referenced(1). From the corresponding P-value, it was shown that in the tested variables, the B-acidity and A-temprecture value had the greatest influence on the removal efficiency of FA, and the surface effect of factor B^2 on the FA removal effect is significant.

The correlation system R^2 is an important reference for the degree of fit. When R^2 tends to be unified, the fit of the empirical model of the actual data is better. Joglekar and Ma(9) suggested that for a good fit of the model, R^2 should be at least 0.80. The R^2 value of this model was 0.9359, indicating that the regression model fits well with the experiment.

Table 5 ANOVA for the regression quadratic model of CCD design

Source	Sum of Squares	Df	Mean Square	F Value	P-value	
Model	5405.22	4	1351.31	29.21	< 0.0001	significant
A-Temperature	2029.59	1	2029.59	43.87	0.0002	
B-Acidity	2208.68	1	2208.68	47.74	0.0001	
A^2	311.26	1	311.26	6. 73	0.0319	
B^2	2679.40	1	2679.40	57. 92	< 0. 0001	
Residual	370.11	8	46.26			
Lack of Fit	304.72	4	76.18	4.66	0.0826	not significant
R-Squared			0.9359			
Adj R-Squared			0.9039			

RSM analysis

Fig 3 is a response surface graph and its contour plots from the multiple regression equation (3). It could be seen that the 3D response surface graph presents an inverted "U" shape, and a "red peak" appears at the center of the right side, meaning that the target optimal response value is obtained near here(11). In the case of a fixed temperature, the target response value first increases and then tends to be gradual, and finally decreases slowly. On the other hand, if the acidity value fixed, the target response value increases slowly with increasing temperature, and the increase is small. This also showed that the degree of influence of acidity on the target FA removal was greater than temperature. The shape of the contour plots indicates the nature and extent of the interaction. The regular elliptical nature of the contour plots shows significant interactions, while the near-circular nature of the contour plots shows less prominent or negligible interactions(20) .It could be seen from the contour plot of Fig 3 that there is no strong interaction between the influencing factors A and B here, which is consistent with the results obtained by the ANOVA above(Tab. 5). From the contour plots, the optimal acid of the model could be obtained in the acid pH range of 3 to 5, whereas the optimal temperature could not be found, it might be over 90°C, so the model did need further optimization.

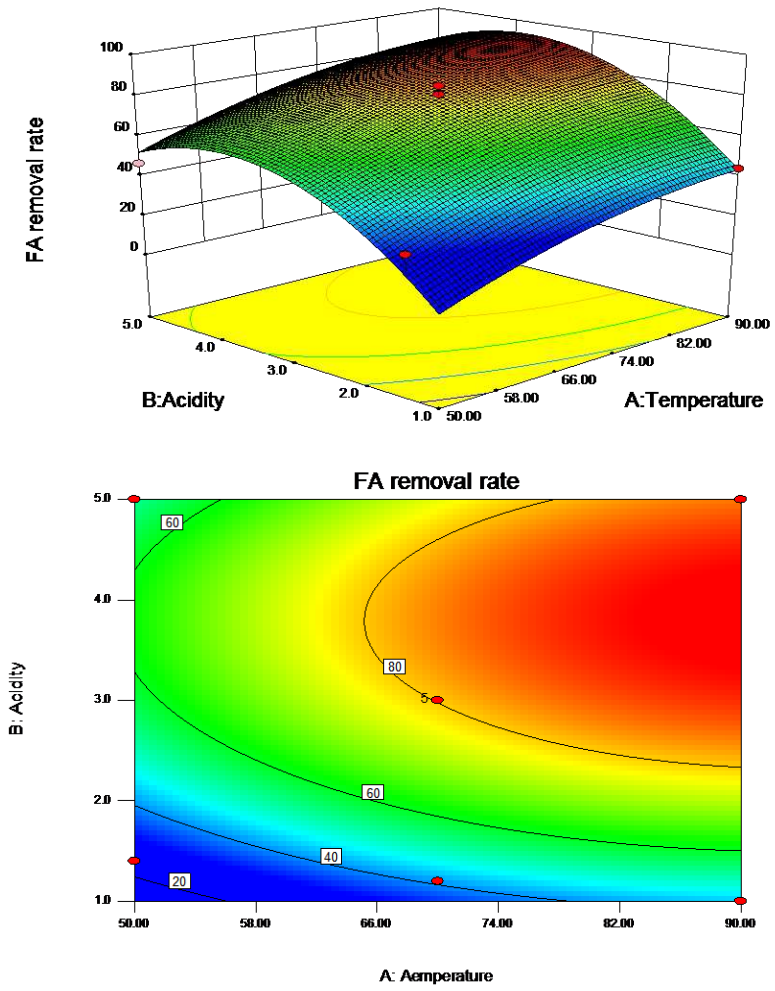

Fig. 3 3D response surface graph and contour plots

Optimization of influencing factors

The main purpose of the optimization was to determine the optimal parameter values for maximizing the FA removal, therefore, the maximum removal of FA was selected as the target value. Since the optimal tempreture may be emerged over 90°C, the tempreture range was enlarge from 60-90°C to 60-130°C. Then the optimum values were obtained, as shown in Fig.4, whereby two optimization schemes were also obtained in Table 6. Since the conditions of the two schemes were very close, and the expected target values are not different from each other, the temperature and acidity were finally selected as 94°C and pH = 3.8 respectively for the convenience of the experimental conditions setting.

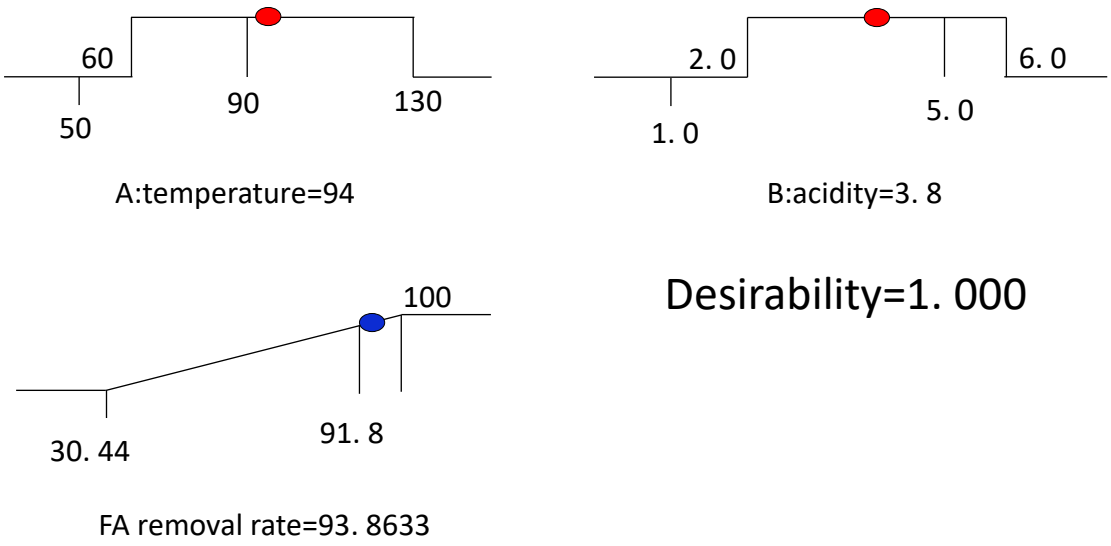

Fig.4 Desirable slope for numerical optimization of the CWPO conditions

Table 6 RSM system optimized solution

Solution	Temperature	Acidity	FA removal rate(%)	Desirability
1	94.07	3.8	93.8643	1.000
2	93.99	3.8	93.8622	1.000
Predition	94	3.8	93. 8633	1.000

Fig 5 is the optimized 3D surface graph and contour plots. Compared with Fig.3, a mountain shape 3D surface graph was obtained and it was obvious that the maxmum removal of FA(93.8633%) was at the peak of the mountain.

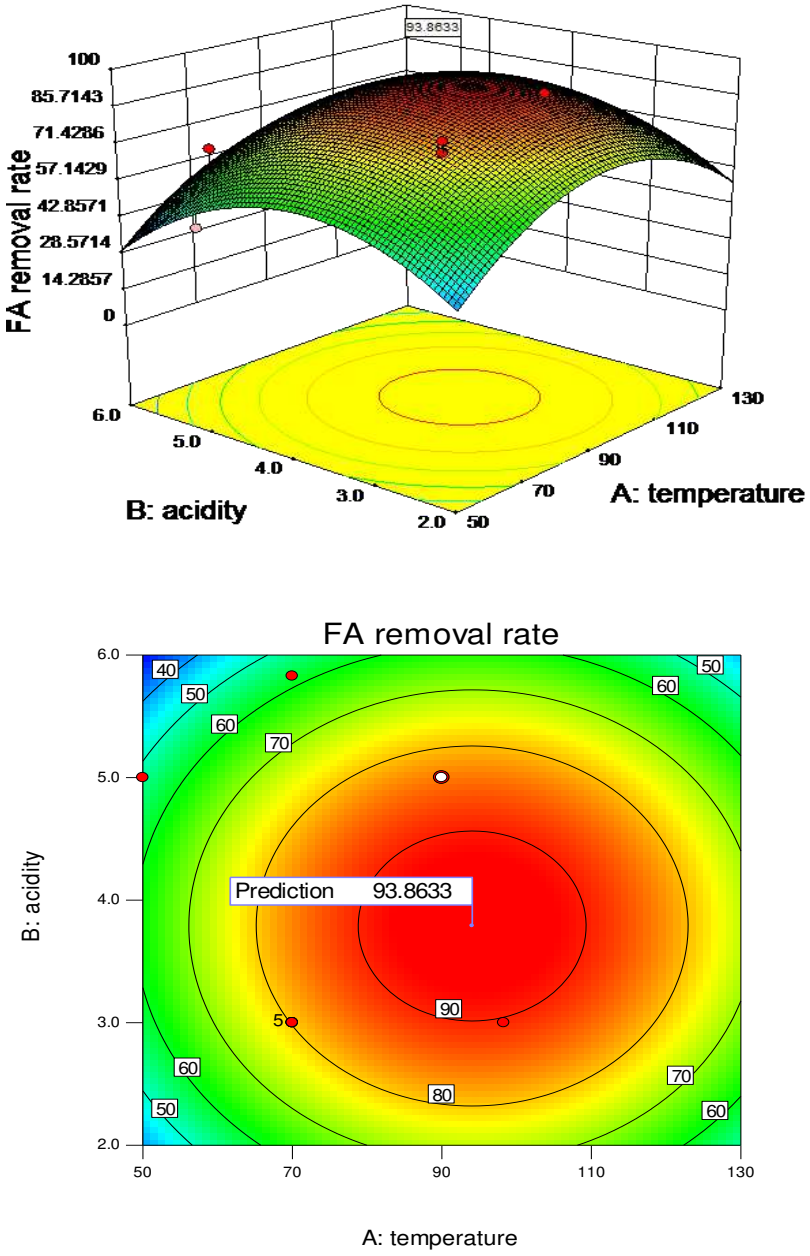

Fig. 5 Optimized 3D surface graph and contour plots

Results verification

To confirm whether the model is sufficient to predict the maximum FA removal efficiency, three repetitive tests were performed under the optimal operating condition as shown in Table 7. The average maximum FA removal efficiency produced by three replicate experiments was 93.02%, while the RSM optimal target response was 93. 86%. The good agreement between the predicted results and the experimental results verifies the validity of the model and confirms that CCD-RSM is a powerful tool for optimizing the experimental factors.

Table 7 Optimum value of the process parameter for maximum efficiency

Parameter		Y(remocal efficiency, %)		
	Times	1	2	3
practice	Single	92.45	92.82	93.78
	Average		93.02	
Predition			93.86	

Removal efficiency under different systems

The removal rates of FA, TOC, and CN expressed by α, β, and γ respectively were shown in Fig.6. It can be seen from the figure that the addition of oxidant H_2O_2 is crucial. The experimental groups with H_2O_2 added(the latter tree groups) had better removal rates of FA, TOC and CN compared to the experimental group without H_2O_2(the former two groups in Fig.6). Among the latter three groups, the groups with catalyst achieved higher removal rate than the group without catalyst. The removal rates of the three indicators had increased, especially the removal rate of TOC had improved significantly, from 13.2% to 81.9%, which indicates that the addition of ZVC could greatly increase the mineralization rate of FA in the CWPO reaction. Under the same condition, the mineralization rate was near 2.5 times higher than that of the experimental group without ZVC., ZVC also has obvious effects on FA degradation and color removal. All the results shows that the ZVC / CTS-ACB catalyst prepared in this paper has high catalytic activity in FA removal and organic compound mineralization.

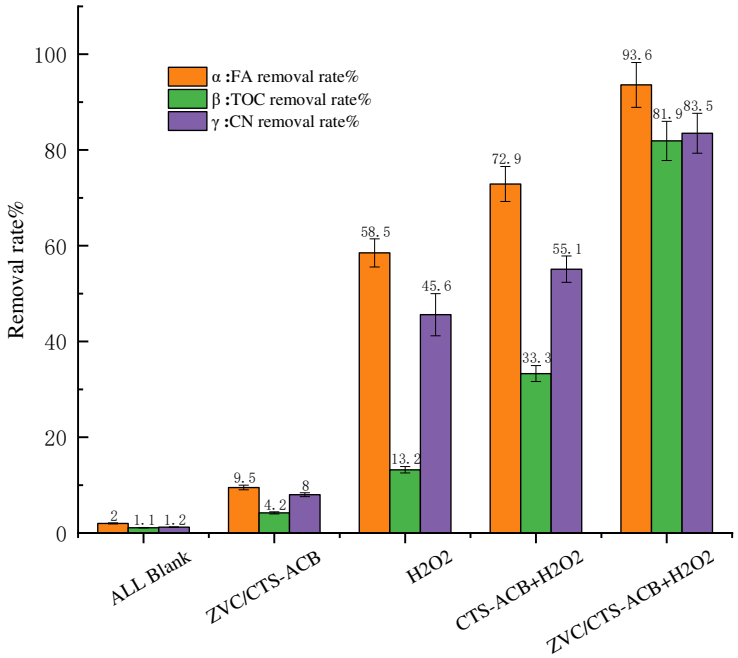

Fig. 6 Catalyst and oxidant controlled trials. FA=100mg·L^{-1},

temperature=94°C, time=90min, pH=3.8, CTS-ACB and ZVC/CTS-ACB=4g·L^{-1}, H_2O_2=20mmol.

Conclusion and outlook

This study demonstrates the applicability of the prepared ZVC/CTS-ACB to the degradation of FA in CWPO. The statistical tool Plackett-Buiman and central composite design coupled with the response surface model were used to analyze the experimental data and predict the optimal target response value. Under the optimal conditions given by the system, the experiment was repeated three times. The removal rate of FA was 93.02%, which was very close to the predicted target response value of 93.86%, indicating that the model was established accurately. The experiment results comfirm that the PB experiment and the CCD-RSM are suitable for optimizing the operating conditions in a multi-factor operating environment to obtain the maximum FA degradation rate. Catalyst and oxidant comparison experimental results showed that the catalyst and oxidant were essential factors in the CWPO reaction. The ZVC/CTS-ACB catalyst could greatly increase the mineralization rate of FA. The TOC removal rate of 81.9% indicated that most of FA were directly mineralized into CO_2 and H_2O during the CWPO process, in which ZVC/CTS-ACB showed the high catalytic activity. Further study will be conducted on the catalytic mechanism of ZVC/CTS-ACS to FA removal and application of the catalyst in leachate treatment with CWPO.

References:

[1] Abdulredha, M. M., S. A. Hussain & L. C. Abdullah (2020) Optimization of the demulsification of water in oil emulsion via non-ionic surfactant by the response surface methods. *Journal of Petroleum Science and Engineering,* 184**,** 106463.

[2] Abecassis-Wolfovich, M., M. V. Landau, A. Brenner & M. Herskowitz (2004) Catalytic Wet Oxidation of Phenol with Mn−Ce-Based Oxide Catalysts: Impact of Reactive Adsorption on TOC Removal. *Industrial & Engineering Chemistry Research,* 43**,** 5089-5097.

[3] Aiken, G. R., H. Hsu-Kim & J. N. Ryan (2011) Influence of Dissolved Organic Matter on the Environmental Fate of Metals, Nanoparticles, and Colloids. *Environmental Science & Technology,* 45**,** 3196-3201.

[4] Amiri, A. & M. R. Sabour (2014) Multi-response optimization of Fenton process for applicability assessment in landfill leachate treatment. *Waste Management,* 34**,** 2528-2536.

[5] An, W., Q. Zhang, Y. Ma & K. T. Chuang (2001) Pd-based catalysts for catalytic wet oxidation of combined Kraft pulp mill effluents in a trickle bed reactor. *Catalysis Today,* 64**,** 289-296.

[6] Casey, T. J. & K. H. Chua (1997) Aspects of THM formation in drinking-water. *Journal of Water Supply: Research and Technology - AQUA,* 46**,** 31-39.

[7] Ding, Y. & X. Xia (2008) Preparation and characterization of hollow carbon nanospheres supported metallic catalysts by using one-step pyrolysis method. *Journal of nanoscience and nanotechnology,* 8**,** 1512-7.

[8] Eftaxias, A., J. Font, A. Fortuny, A. Fabregat & F. Stüber (2006) Catalytic wet air oxidation of phenol over active carbon catalyst: Global kinetic modelling using simulated annealing. *Applied Catalysis B: Environmental,* 67**,** 12-23.

[9] Fu, J., M. Ji, Y. Zhao & L. Wang (2006) Kinetics of aqueous photocatalytic oxidation of fulvic acids in a photocatalysis – ultrafiltration reactor (PUR). *Separation and Purification Technology,* 50**,** 107-113.

[10] Iskander, S. M., R. Zhao, A. Pathak, A. Gupta, A. Pruden, J. T. Novak & Z. He (2018) A review of landfill leachate induced ultraviolet quenching substances: Sources, characteristics, and treatment. *Water Research,* 145**,** 297-311.

[11] Kim, S. (2016) Application of response surface method as an experimental design to optimize coagulation – flocculation process for pre-treating paper wastewater. *Journal of Industrial and Engineering Chemistry,* 38**,** 93-102.

[12] Luan, M., G. Jing, X. Xu, B. Hou, Y. Wang & D. Meng (2013) A Review: Wet Oxidation and Catalytic Wet Oxidation of Industrial Wastewater. *Recent Patents on Chemical Engineering,* 6.

[13] Milone, C., A. R. Shahul Hameed, E. Piperopoulos, S. Santangelo, M. Lanza & S. Galvagno (2011) Catalytic Wet Air Oxidation of p-Coumaric Acid over Carbon Nanotubes and Activated Carbon. *Industrial & Engineering Chemistry Research,* 50**,** 9043-9053.

[14] Morales, J., J. A. Manso, A. Cid & J. C. Mejuto (2012) Degradation of carbofuran and carbofuran-derivatives in presence of humic substances under basic conditions. *Chemosphere,* 89**,** 1267-1271.

[15] --- (1946) The Design of Optimum Multifactorial Experiments. *Biometrika,* 33**,** 305-325.

[16] Poznyak, T., G. L. Bautista, I. Chaírez, R. I. Córdova & L. E. Ríos (2008) Decomposition of toxic pollutants in landfill leachate by ozone after coagulation treatment. *Journal of Hazardous Materials,* 152**,** 1108-1114.

[17] Rivas, J., F. Beltrán, M. D. F. Carvalho & P. Alvarez (2005) Oxone-Promoted Wet Air Oxidation of Landfill Leachates. *Industrial & Engineering Chemistry Research - IND ENG CHEM RES,* 44.

[18] Tang, W., G. Zeng, J. Gong, J. Liang, P. Xu, C. Zhang & B. Huang (2014) Impact of humic/fulvic acid on the removal of heavy metals from aqueous solutions using nanomaterials: A review. *Science of The Total Environment,* 468-469**,** 1014-1027.

[19] Tizaoui, C., L. Bouselmi, L. Mansouri & A. Ghrabi (2007) Landfill leachate treatment with ozone and ozone/hydrogen peroxide systems. *Journal of Hazardous Materials,* 140**,** 316-324.

[20] Wang, J., Y. Chen, Y. Wang, S. Yuan & H. Yu (2011) Optimization of the coagulation-flocculation process for pulp mill wastewater treatment using a combination of uniform design and response surface methodology. *Water Research,* 45**,** 5633-5640.

[21] Wang, J., Y. Zhou, A. Li & L. Xu (2010) Adsorption of humic acid by bi-functional resin JN-10 and the effect of alkali-earth metal ions on the adsorption. *Journal of Hazardous Materials,* 176**,** 1018-

1026.

[22] Wang, S., X. Sun, X. Liu, W. Gong, B. Gao & N. Bao (2008) Chitosan hydrogel beads for fulvic acid adsorption: Behaviors and mechanisms. *Chemical Engineering Journal,* 142**,** 239-247.

[23] Wen, G., S. Wang, J. Ma, T. Huang, Z. Liu, L. Zhao & J. Xu (2014) Oxidative degradation of organic pollutants in aqueous solution using zero valent copper under aerobic atmosphere condition. *Journal of Hazardous Materials,* 275**,** 193-199.

[24] Weuster-Botz, D. (2000) Experimental design for fermentation media development: Statistical design or global random search? *Journal of Bioscience and Bioengineering,* 90**,** 473-483.

[25] Zhang, Y., J. Fan, B. Yang, W. Huang & L. Ma (2017) Copper‐catalyzed activation of molecular oxygen for oxidative destruction of acetaminophen: The mechanism and superoxide-mediated cycling of copper species. *Chemosphere,* 166**,** 89-95.

[26] Zhao, L., F. Luo, J. M. Wasikiewicz, H. Mitomo, N. Nagasawa, T. Yagi, M. Tamada & F. Yoshii (2008) Adsorption of humic acid from aqueous solution onto irradiation-crosslinked carboxymethylchitosan. *Bioresource Technology,* 99**,** 1911-1917.

[27] Zhou, P., J. Zhang, Y. Zhang, J. Liang, Y. Liu, B. Liu & W. Zhang (2016) Activation of hydrogen peroxide during the corrosion of nanoscale zero valent copper in acidic solution. *Journal of Molecular Catalysis A: Chemical,* 424**,** 115-120.

Figures

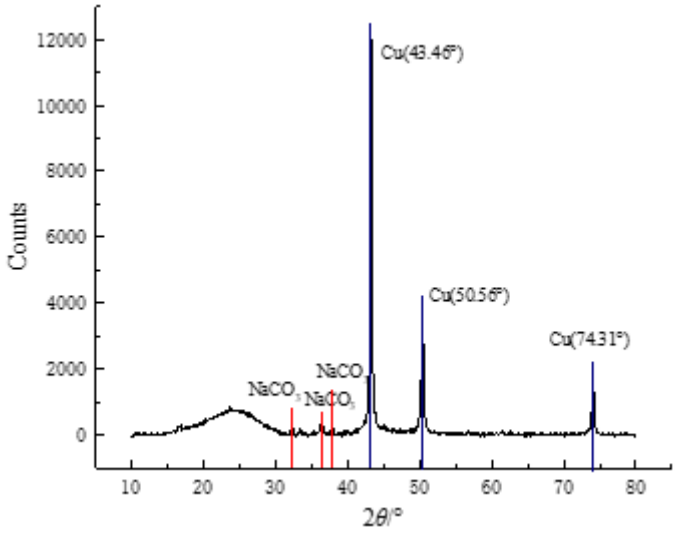

Figure 1

XRD pattern of ZVC/CTS-ACB

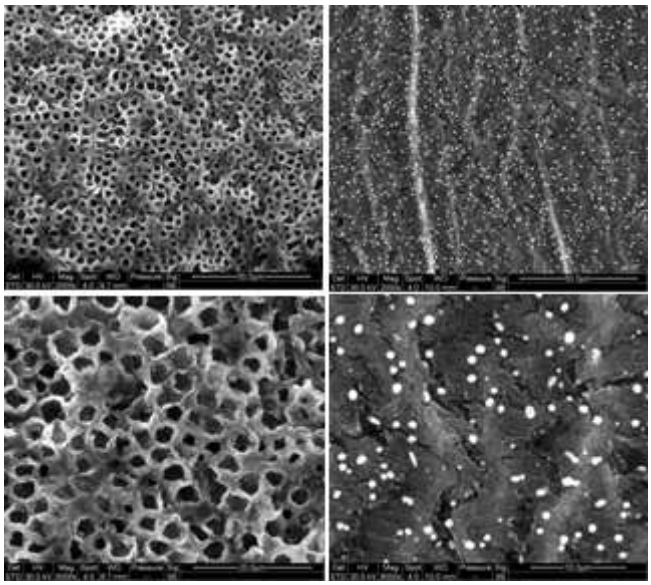

Figure 2

SEM micrograph of external and internal cross-section of ZVC/CTS-ACB (a.outer surface is magnified 2,000 times, b.outer surface is magnified 5,000 times, c.inner cut surface is magnified 2,000 times, d inner cut surface is magnified 8,000 times)

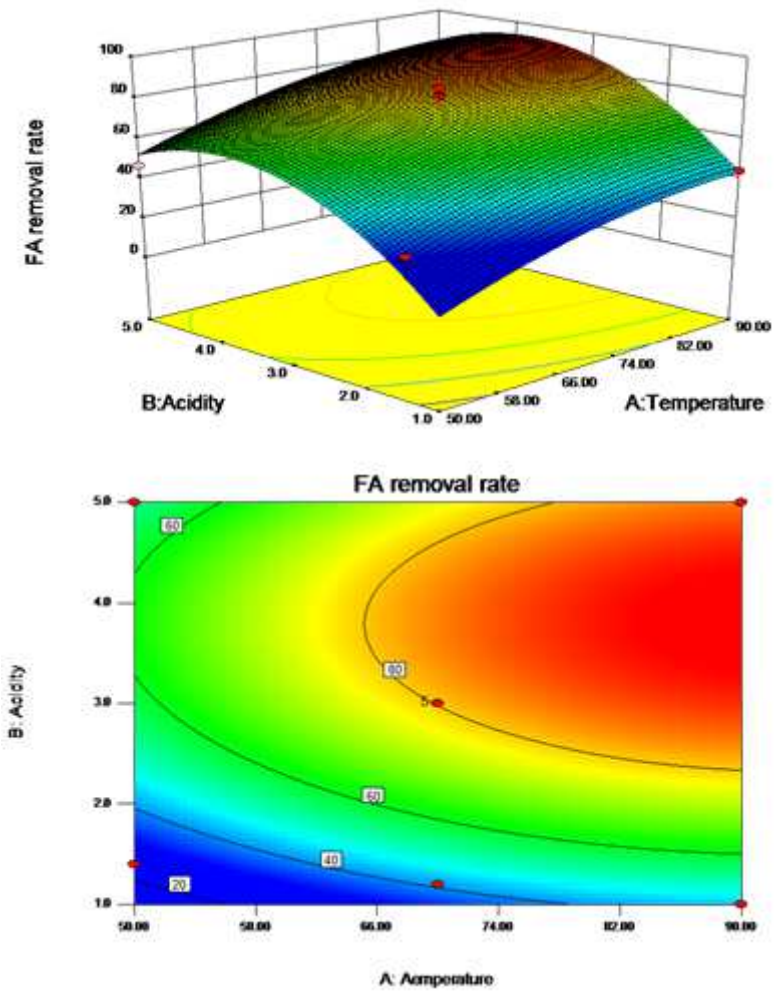

Figure 3

3D response surface graph and contour plots

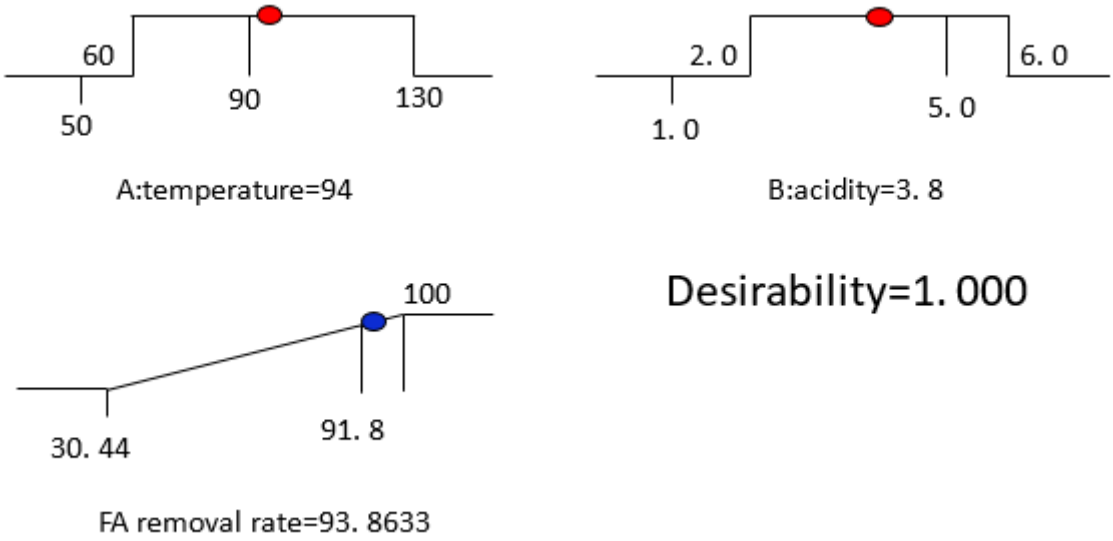

Figure 4

Desirable slope for numerical optimization of the CWPO conditions

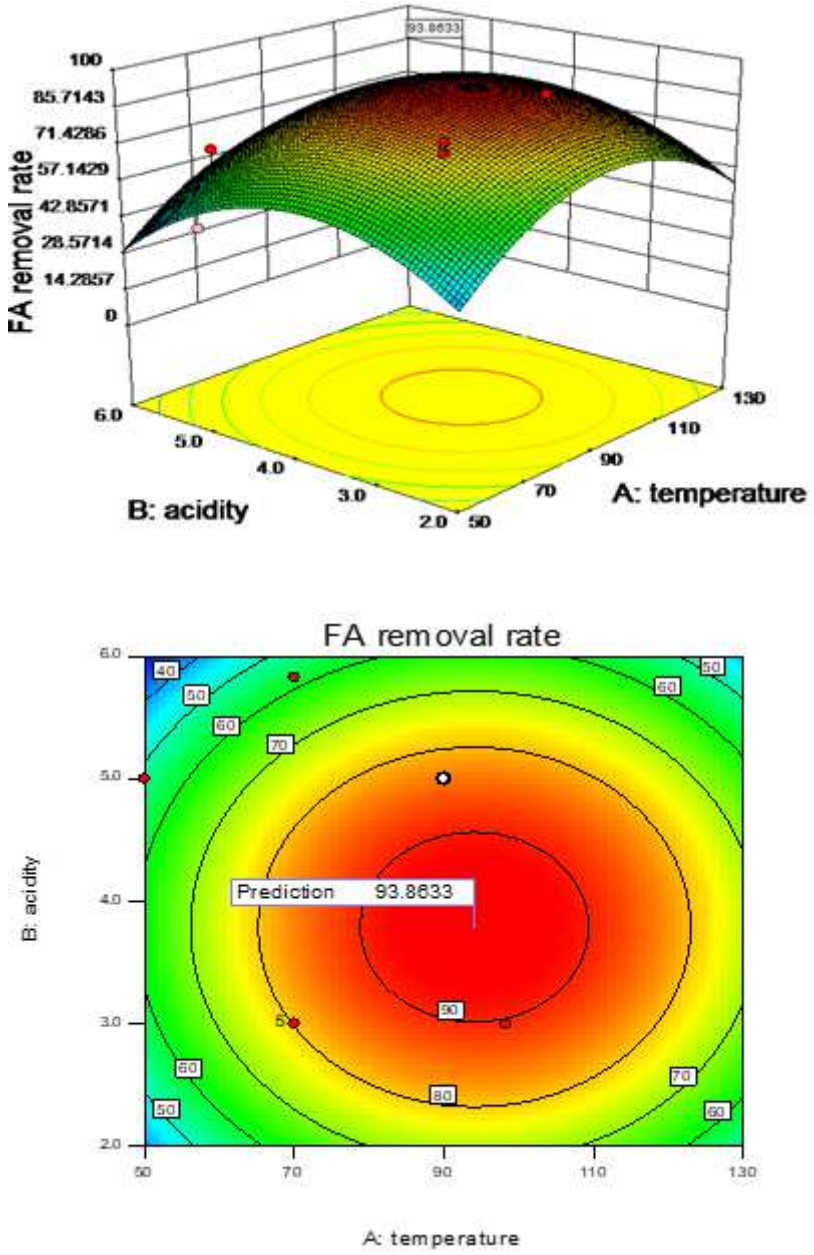

Figure 5

Optimized 3D surface graph and contour plots

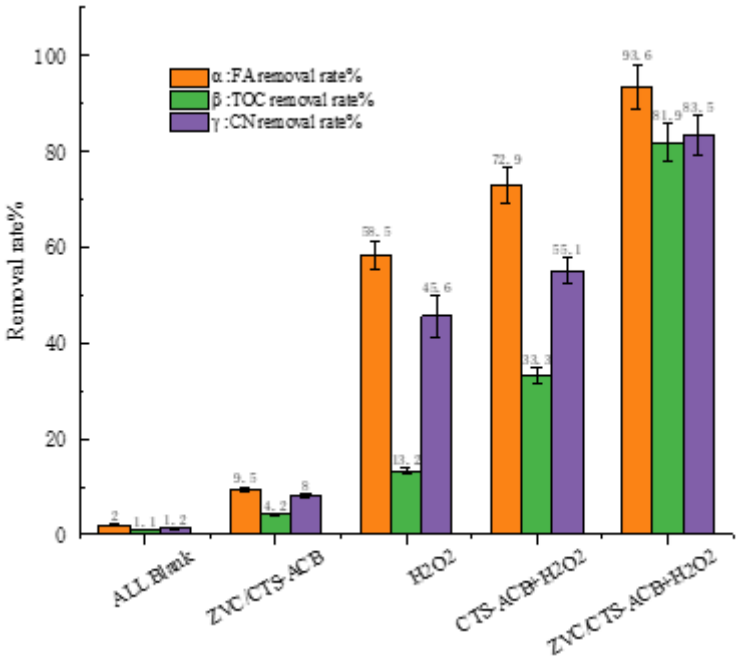

Figure 6

Catalyst and oxidant controlled trials. FA=100mg·L-1, temperature=94□C, time=90min, pH=3.8, CTS-ACB and ZVC/CTS-ACB=4g·L-1, H2O2=20mmol.